

Heat capacity of a thermally squeezed optomechanical oscillator at strong coupling

Michal Kolář,¹ Artem Ryabov,² and Radim Filip¹

¹*Palacký University, Department of Optics, 17. listopadu 1192/12, 771 46 Olomouc, Czech Republic*

²*Charles University, Faculty of Mathematics and Physics,*

Department of Macromolecular Physics, V Holešovičkách 2, 180 00 Praha 8, Czech Republic

(Dated: July 19, 2022)

Coherent quantum oscillators are basic physical system both in quantum statistical physics and quantum thermodynamics. We discuss and compare two thermodynamic coefficients (generalized heat capacities) characterizing optomechanical oscillator strongly coupled to a thermal bath. The coupling is strong enough for the observed oscillator energy levels to be dependent on bath temperature. The capacities are related to two different experiments. One measurement is a differential scanning calorimetry, the second probes the second statistical moment of the oscillator position. As we analyze, the strong coupling allows both localization and purification of the oscillator induced by increasing the bath temperature. The capacities can be negative and can witness certain types of the energy-levels temperature dependence. Our findings are stimulating for current development of optomechanical and thermomechanical experiments.

I. INTRODUCTION

Quantum optomechanics and electromechanics becomes a physical bridge between developed atomic, molecular and optical physics and emerging quantum thermodynamics. It is due to possibility to operate mechanical and electrical oscillators as quantum systems [1] as well as to understand them as a part of thermodynamical processes and engines [2]. The oscillator can generate parametric oscillations, when the oscillation frequency is periodically controlled [3]. Such parametric oscillators are capable to squeeze the noise below the ground state of that mechanical oscillator [4]. The solid-state nature of these oscillators simultaneously implies that the basic characteristics of their modes (such as mode frequencies) can be strongly influenced by ambient temperature [5–9]. Despite the fact that this sensitive dependence can make them promising temperature sensors [10], on a more fundamental level, it opens the doors towards experimental investigation of thermodynamics of quantum mechanical systems strongly coupled to their environment.

A number of general theoretical thermodynamic studies of strongly coupled systems appeared recently [11–19] (for classical works see Refs. [20, 21]). However, a fundamental theoretical approach encounters severe difficulties, e.g., how to unambiguously define thermodynamic quantities on a microscopic level [19]. A promising way to resolve these theoretical struggles is to propose and build in the lab real-world quantum-mechanical thermodynamic devices. After such experiments, quantum thermodynamics can develop to describe new effects available due to quantum engineering.

Therefore, contrary to the fundamental theoretical effort, in this work we have chosen an experimentally-oriented approach. We propose two experiments on an oscillator whose frequency depends on temperature T . Each experiment is described by the corresponding heat capacity. The first utilizes a reconstruction procedure of the system density matrix [22], while the second one is a quantum analogue of the differential scanning calorimetry [23]. For energies of the mode we assume

$$E_n(T) = \hbar\omega(T) \left(n + \frac{1}{2} \right), \quad (1)$$

where the mode frequency is obtained from $\omega^2(T) = \omega_0^2 + f(T)$, ω_0 being the bare oscillator frequency and T the bath temperature. Hence, the oscillator energy levels are temperature-dependent (for various aspects of thermodynamics of systems with temperature-dependent energy levels we refer to works [11, 20, 21, 24–33]). The bare oscillator frequency ω_0 is a temperature-independent constant. Interaction with environmental degrees of freedom changes phenomenologically the bare frequency through the function $f(T)$. Simultaneously, the environment equilibrates the oscillator at temperature T , cf. Fig. 1. Therefore, the effect of a change of temperature is now principally different from previously studied cases of the sole frequency change in a temperature-stable environment. We assume the polynomial form of this function

$$f(T) = \sum_{k=1}^{\Omega} a_k T^k, \quad (2)$$

with Ω being the maximum order up to which we truncate the series expanding $f(T)$ in T . In modeling optomechanical oscillators, frequently only weak linear dependence on temperature is considered [6], which is valid for small frequency

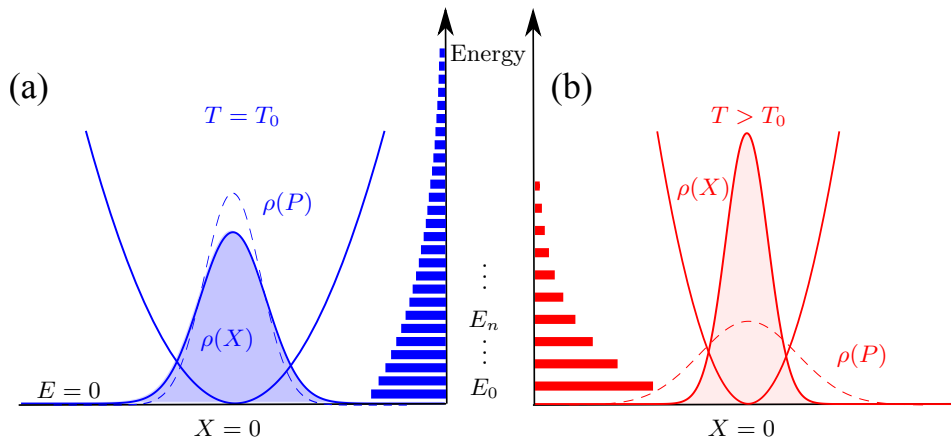


FIG. 1. Thermal squeezing of the optomechanical oscillator strongly coupled to a heat bath. (a) The oscillator in contact with a heat bath (lower temperature T_0 , blue) is described by the Hamiltonian $\hat{H}(T_0)$, Eq. (3), initially. (b) Later, the temperature of the heat bath is increased to $T > T_0$, as indicated (red). The Hamiltonian changes correspondingly to $\hat{H}(T)$, together with the oscillator state, schematically showing the reduction of the variance (*localisation*) of the position distribution $\rho(X)$ (shaded) with increasing temperature and the increase of the momentum distribution (dashed) $\rho(P)$, discussed in Sec. III. The horizontal bars represent the populations of the energy eigenstates for respective potentials. They show schematically the reduction of the von Neumann entropy with increasing temperature (*purification* of the state), discussed in Sec. IV. These effects of statistical physics are responsible for the behavior of the capacities discussed in Sec. V.

shifts. Yet, for large frequency shifts the dependence of frequency on temperature is usually a rather complicated function [10]. In this work we therefore drop this linearization assumption and discuss the consequences of taking the higher order terms into account. In discussed examples we assume the maximum order of the temperature dependence in the range $0 < \Omega \leq 3$. For first-principle derivation of frequency shifts we refer to works [34–36].

The temperature-dependent spectrum (1) represents eigenvalues of the so-called Hamiltonian of the mean force \hat{H} (the term derived from the potential of the mean force originally introduced in theory of fluids [37–39]),

$$\hat{H}(T) = \frac{\hat{P}^2}{2m} + \frac{m}{2} [\omega_0^2 + f(T)] \hat{X}^2, \quad (3)$$

m being the oscillator constant (effective) mass. We prescribe the Hamiltonian of the mean force directly, without its microscopic derivation. Hence our approach is phenomenological. As such it is valid for a broad class of systems. Explicit first-principle calculations of thermodynamic functions for the temperature independent oscillator can be found in Refs. [40–42], for discussion of specific heats see [43, 44].

In Sec. II we introduce the Hamiltonian of mean force and the thermal state oscillator of the generated by it. Section III discusses the mechanical equilibrium properties of the system, namely the temperature dependence of the position variance of the oscillator. In Sec. IV we study the temperature dependence of the von Neumann entropy, particularly its decrease with increasing bath temperature. Section V analyses the temperature dependence of two thermodynamic coefficients and their mutual connection. In Sec. VI we conclude our results. We show that such temperature-dependent energy spectrum of the oscillator can cause reduction of the position variance or of the von Neumann entropy with *increasing* temperature, as well as *negative* heat capacities.

II. PHENOMENOLOGICAL APPROACH TO STRONG COUPLING

The total Hamiltonian of the oscillator interacting with the heat bath reads

$$\hat{H}_{\text{tot}} = \hat{H}_0 + \lambda \hat{H}_I + \hat{H}_B, \quad (4)$$

where the dimensionless parameter λ reflects the system-bath coupling strength. When the interaction $\lambda \hat{H}_I$ between the bare oscillator Hamiltonian \hat{H}_0 and the equilibrium heat bath \hat{H}_B is weak, the oscillator is known to thermalize into the Gibbs canonical state, $\hat{\rho}_G(T) \sim \exp[-\hat{H}_0/k_B T]$ [45]. On the other hand, for a strong coupling, the state of the oscillator will depend on parameters (other than only T) of the ambient environment, even in the long-time limit.

However, even for the strong coupling case, the equilibrium state of the oscillator can still be formally considered in the canonical form determined by the bath temperature T

$$\hat{\rho}(T) = \frac{1}{Z(T)} \exp \left[-\hat{H}(T)/k_B T \right], \quad (5)$$

where the operator $\hat{H}(T)$ is known as the Hamiltonian of mean force (HMF) [16, 18, 19], and $Z(T)$ is the partition function, $Z(T) = \text{Tr} \left[\exp \left[-\hat{H}(T)/k_B T \right] \right]$.

The HMF is obtained after averaging over bath degrees of freedom in the total system as follows [16, 18, 19]

$$\hat{H}(T) = \hat{H}_0 - k_B T \ln \left\langle e^{-\lambda \hat{H}_I/k_B T} \right\rangle_{\text{B}}. \quad (6)$$

The second term on the right-hand side of Eq. (6) contains all details of the interaction between the system and bath and depends on the parameters of the bath itself (e.g., spectrum of its phonon modes). Within our phenomenological approach, all these details are incorporated into the function $f(T)$ that describes the temperature-dependent shift of the frequency $\omega^2(T) = \omega_0^2 + f(T)$. The HMF (3) assumed in the present work covers a broad class of models of the strongly coupled oscillators with temperature-dependent frequency.

III. TEMPERATURE-INDUCED LOCALIZATION

Thorough understanding of mechanical characteristics is crucial for a physical insight into different equilibrium thermodynamic properties of states (5), discussed in the next section, modified by temperature-dependent frequency shift as given in Eq. (3). In quantum opto-mechanical experiments it is typically a single variable, $\cos(\theta)\hat{X} + \sin(\theta)\hat{P}$, of the oscillator that is being indirectly measured [1]. The position of oscillating microparticles and nanoparticles can be measured in the experiments with nonlinear optical tweezers [46].

In this section we discuss the outcome of such a measurement, namely the variance of the quadrature \hat{X} , $\text{Var}_X(T)$. For different forms of the frequency shift function $f(T)$, defined in Eq. (2), we obtain qualitatively different temperature dependencies of the position variance. For certain parameters, we observe the position *localization* when increasing T . In Sec. IV, the localization will be generalized to the *purification* of the state, i.e. the entropy reduction, where its measurement and the thermodynamic consequences will be discussed. Interestingly, the localization does not necessarily implies the purification of the state.

For the thermal state (5), the quantum mechanical result for the variance of the quadrature \hat{X} reads

$$\text{Var}_X(T) = \frac{\hbar}{m\omega(T)} \left(\langle \hat{n} \rangle + \frac{1}{2} \right), \quad (7)$$

where $\langle \hat{n} \rangle = [\exp(\hbar\omega(T)/k_B T) - 1]^{-1}$ is the Bose-Einstein thermal population of the oscillator mode. Therefore, the temperature-dependent frequency enters both the thermal population and the ground state variance for $\langle \hat{n} \rangle = 0$. It makes a localization of the system nonlinear even for linear change of $\omega(T)$ over the temperature.

In the current experiments, temperature of environment keeps the oscillator in the equilibrium still far away from the ground state [1]. Therefore we primarily focus on a high-temperature limit $\hbar\omega(T)/k_B T \ll 1$. In this limit, variances of position and momentum are given by

$$\text{Var}_X(T) \approx \frac{k_B T}{m\omega^2(T)}, \quad \text{Var}_P(T) \approx mk_B T, \quad (8)$$

respectively. Apparently, the momentum variance $\text{Var}_P(T)$ does not depend on $\omega(T)$ and it behaves just as for the system weakly coupled to a bath. It however depends on temperature T and therefore, it will influence other quantities, e.g. entropy, when T changes. If the frequency does not depend on temperature, $\omega(T) = \omega_0$, the variance $\text{Var}_X(T)$ increases linearly with T , and the oscillator exhibits *thermal delocalization*.

Eqs. (8) are valid in the high-temperature limit $\hbar\omega(T)/k_B T \ll 1$. Our system reaches this limit and stays there for appropriate parameter values in equation (2): $\Omega \leq 3$, $a_\Omega < 0$, or $\Omega \leq 2$, $a_\Omega > 0$ for almost any T , except the region of extremely small bath temperatures (not attainable in current optomechanical and electromechanical experiments [1]). This behavior is clear for $a_\Omega \leq 0$. For $a_\Omega > 0$ is caused by the decrease of the ratio $\omega(T)/T$ for increasing temperature of the bath. Even-though the energy level separation $\hbar\omega(T)$ increases with T , the average thermal energy $k_B T$ increases faster, thus still allowing for the average thermal population increase. On contrary, in the case $a_3 > 0$ the relative increase of $\omega(T)/T$ might bring the oscillator out of Eq. (8) validity regime for increasing

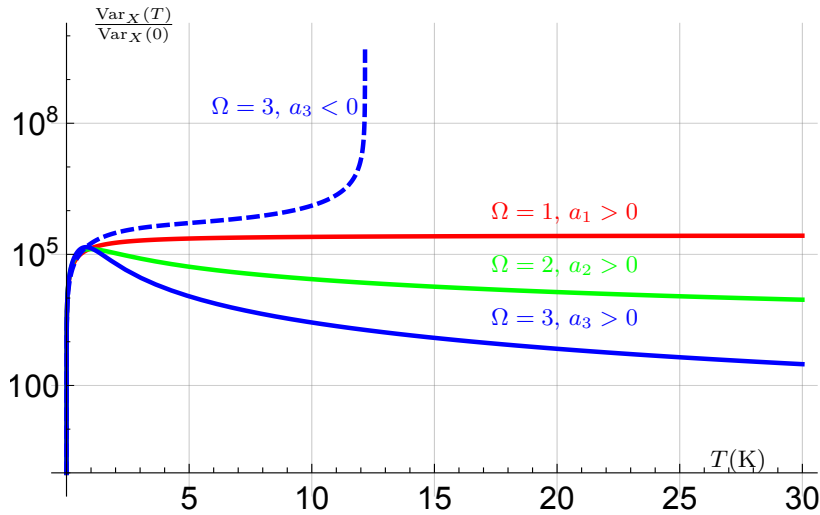


FIG. 2. The semi-logarithmic plot of the normalized variance of the oscillator position, $\text{Var}_X(T)/\text{Var}_X(0)$ Eq. (7), for different values of the parameters in Eq. (2). For all curves the parameters plotted correspond to the deep classical regime, $\hbar\omega(T)/k_B T \ll 1$ (parameters inspired by recent experiments [46]). For negative coefficients $a_\Omega < 0$ the variances diverge for large enough T , as illustrated by the blue-dashed curve for typical example $a_3 < 0$. The behavior for $a_\Omega > 0$ is shown by full lines. The red and green curves correspond asymptotically (for large enough T) to the deep classical regime of the oscillator, $\hbar\omega(T)/k_B T \ll 1$, while having different asymptotics. The red curve saturates, while the green decreases as $\sim T^{-1}$. It witnesses *thermal steady-state localization*. The blue-full curve corresponds to $\Omega = 3$, $a_3 > 0$. In the regime plotted, the variance decreases as $\text{Var}_X(T) \sim T^{-2}$. The parameters values used in these plots are $m \approx 10^{-8}$ kg, $\omega_0 \approx 10^6$ rad/s, $|a_\Omega T^\Omega| \approx \omega_0^2$ for all cases.

temperature. Physically, this corresponds to the situation in which $\omega(T)$ increases fast enough, so that the bath is less able to excite the temperature dependent inter-level energy difference $\hbar\omega(T)$ with the typical thermal energy $k_B T$. Such situation may bring the oscillator effectively closer to the ground state for increasing temperatures. This case, however, does not appear for the experimentally motivated parameters used in the present work.

For $\Omega \leq 3$, $a_\Omega < 0$, the variance (8) diverges at $T_d \approx \sqrt[\Omega]{\omega_0^2/|a_\Omega|}$, see the dashed line in Fig. 2. Such behavior is caused by $\omega(T_d) = 0$, meaning the confining potential disappears at $T = T_d$, while the oscillator becomes a free particle. Qualitatively different effects can be found for $\Omega \leq 2$, $a_\Omega > 0$.

For $\Omega = 1$, $0 < a_1$, the variance saturates at $\text{Var}_X(T) = k_B/(ma_1)$ for large enough temperatures, see the red curve in Fig. 2. In this case, the temperature dependence of $\omega^2(T)$ becomes linear for high enough temperatures satisfying $a_1 T \gg \omega_0^2$, canceling exactly the numerator in $\text{Var}_X(T)$. $\text{Var}_X(T)$ never exceeds this limiting value.

In the case $\Omega = 2$, $0 < a_2 \ll k_B^2/\hbar^2$ we find $\text{Var}_X(T)$ decreasing as $\text{Var}_X(T) \sim T^{-1}$ for large enough temperatures satisfying $a_2 T^2 \gg \omega_0^2$, see the green line in Fig. 2. This is caused by the quadratic increase of the denominator of (8) and linear increase of its nominator. Interestingly, this behavior does not oppose the fact that the oscillator still remains in the classical domain $\hbar\omega(T)/k_B T \ll 1$ due to $\omega(T)/T \sim 1$ for $a_2 T^2 \gg \omega_0^2$. Despite the oscillator stays in the classical regime, we observe an anomalous behavior – *thermal localization* due to strong coupling with the heat bath.

The value $\Omega = 3$ reveals yet another qualitatively different behavior. We find again $\text{Var}_X(T) \rightarrow 0$, being approached as $\text{Var}_X(T) \sim T^{-2}$, see the blue line in Fig. 2, due to the cubic increase of the denominator of (8) and linear increase of its nominator. On contrary to the previous case $\Omega = 2$, the oscillator aims to the quantum regime $\hbar\omega(T)/k_B T \approx 1$ due to the dependence $\omega(T)/T \sim T^{1/2}$ for $a_3 T^3 \gg \omega_0^2$.

By inspection, $\text{Var}_X(T)$ is an increasing function of T for low temperatures, meaning

$$\frac{\partial \text{Var}_X(T)}{\partial T} > 0. \quad (9)$$

Eq. (9) and the oscillator localization (in certain cases) for large enough temperatures predicts the existence of a local maximum for the oscillator variance. By definition the maximum variance can not be overcome, in contrast to the common thermal delocalization. The derivative of the position variance in the classical limit (8) with respect to temperature T reads

$$\frac{\partial \text{Var}_X(T)}{\partial T} = \frac{k_B(\omega_0^2 - a_2 T^2 - 2a_3 T^3)}{m\omega^4(T)}, \quad (10)$$

where we have used the notation from Eq. (2). Looking for existence of the $\text{Var}_X(T)$ extreme amounts to finding the roots of the polynomial in the nominator of Eq. (10).

We note that for $\Omega = 1$ the coefficient a_1 does not appear in the nominator of Eq. (10), thus it can only saturate for $a_1 > 0$ as T increases and can not affect the existence of the extrema. This means the extreme does not exist in this case, see Fig. 2. For $a_1 < 0$, Eq. (10) is always positive and $\text{Var}_X(T)$ diverges for $T_d = \sqrt{\omega_0^2/|a_1|}$, the temperature for which $\omega(T_d) = 0$, i.e., the confining potential disappears.

For $\Omega = 2$ the positive root $T_{\max} > 0$ of Eq. (10) nominator exists only for $a_2 > 0$ and reads $T_{\max} = \sqrt{\omega_0^2/a_2}$. The maximum value of $\text{Var}_X(T)$ is then

$$\text{Var}_X(T_{\max}) = \frac{k_B}{m \left[a_1 + 2\sqrt{a_2\omega_0^2} \right]}, \quad (11)$$

meaning that in this regime the position variance can not globally exceed the value of Eq. (11). Notice, T_{\max} increases linearly with frequency, therefore such maximum may be found at high temperature for current high-frequency oscillators [46, 47]. Simultaneously, with increasing frequency the maximum variance (11) decreases, therefore, for its determination the ability to measure small fluctuations of the mechanical oscillator is required.

In the case $\Omega = 3$ finding the roots of Eq. (10) nominator is straightforward but cumbersome. We use here the result for a simplified situation $a_2 \ll a_3 T$, yielding positive root $T_{\max} \approx \sqrt[3]{\omega_0^2/2|a_3|}$. This result is approximately valid if the maximum is reached still in the classical region of parameters. For $a_3 < 0$ the maximum does not exist, $\text{Var}_X(T)$ increases monotonically, and diverges for such T_d for which $\omega(T_d) = 0$, see the blue-dashed line in Fig. 2.

For the last two cases we encounter the aforementioned effect of the *thermal localization* of the oscillator, i.e. the reduction of its position variance, with increasing the bath temperature T . The results of this paragraph suggest that for $\Omega = 3$, $a_3 > 0$, the maximum of the position variance scales with the system frequency as $\text{Var}_X(T_{\max}) \sim \omega_0^{-4/3}$. It is thus preferable to work with higher frequency oscillators if lower values of position variance are the figure of merit.

IV. TEMPERATURE-INDUCED PURIFICATION

In this section we focus on the parallels and remarkable differences between the behavior of the $\text{Var}_X(T)$, reflecting the position *localization*, and the reduction of von Neumann entropy, $S(T)$ (denoted simply as the entropy from now on), of the state (5). The entropy defined in the standard way [45] reads

$$S(T) = -k_B \text{Tr}[\hat{\rho}(T) \ln \hat{\rho}(T)]. \quad (12)$$

The value of $S(T)$ reflects the purity of the oscillator state [48, 49]. Contrary to the position uncertainty quantified solely by $\text{Var}_X(T)$, the state purity depends on both $\text{Var}_X(T)$ and $\text{Var}_P(T)$. To observe the temperature-induced purification (the decrease of $S(T)$ with T), the decrease of uncertainty in the position has to be faster than the increase of momentum uncertainty in the product $\text{Var}_X(T)\text{Var}_P(T)$, completely determining the entropy $S(T)$. To observe such an unusual effect, a more strict condition on $\omega(T)$ must be satisfied compared to the thermally induced localization. In experiment, it requires a precise estimation of the density matrix $\hat{\rho}(T)$, which can be done with the help of the homodyne detection [50].

The approximate result obtained from Eq. (12) using the state (5)

$$S(T) \approx k_B \left[1 - \ln \left(\frac{\hbar\omega(T)}{k_B T} \right) \right], \quad (13)$$

is valid in the *classical limit* $\hbar\omega(T)/k_B T \ll 1$. The entropy of the oscillator is determined solely by the ratio $\hbar\omega(T)/k_B T$, as opposed to the behavior of $\text{Var}_X(T)$, Eq. (8). The temperature dependence of $\omega(T)/T$ dictates the behavior of the entropy, i.e., if $\omega(T)$ grows faster (slower) than linear with T the entropy decreases (increases) with increasing temperature. Due to the monotonicity of the logarithmic function, the local extremes of $\omega(T)/T$ determine the extremes of $S(T)$. The derivative of the approximate result (13)

$$\frac{\partial S(T)}{\partial T} = \frac{k_B(2\omega_0^2 + a_1 T - a_3 T^3)}{2T\omega^2(T)}, \quad (14)$$

yields a relatively simple sufficient condition for existence of entropy extreme with respect to the temperature T .

For $\Omega = 1$, the entropy $S(T)$ has no local extreme, it monotonically increases, meaning the entropy is unbounded from above, see the dashed line in Fig. 3. This is a similar situation as the absence of position variance extreme, discussed in Sec. III. For $a_1 > 0$ the derivative (14) is positive for all T . It is qualitatively similar to the standard case

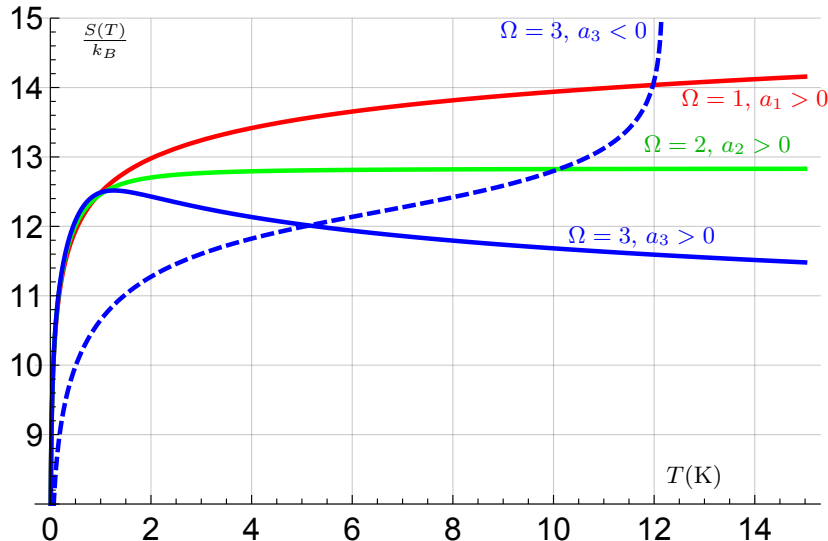


FIG. 3. The entropy Eq. (12) as the function of the temperature for the respective leading-term coefficients a_Ω . For the *negative* coefficient $a_3 < 0$ (blue-dashed) the entropy diverges at points of vanishing $\omega(T)$, $\omega(T_d) = 0$. For *positive* leading-term coefficients a_Ω the behavior depends on the a_Ω value. In the case $\Omega = 1$ (red) the entropy diverges as $S(T) \propto k_B \ln \sqrt{T}$, for $\Omega = 2$ (green) the entropy saturates for large T at the value (15). For $\Omega = 3$ and *positive* leading term coefficients $a_3 > 0$ (blue-full), there exists a local maximum at the temperature $T_{\max} \approx \sqrt[3]{2\omega_0^2/a_3}$ with the maximum value $S(T_{\max})$, Eq. (16). In this regime we observe *thermal purification* of the oscillator and the entropy decreases logarithmically. In all plotted cases $m \approx 10^{-8}$ kg, $|a_\Omega|T \approx \omega_0^2$, $\omega_0 \approx 10^6$ rad/s [46].

of the thermalized linear oscillator coupled weakly to the heat bath. For the negative leading-term coefficient $a_1 < 0$ the maximum does not exist in the $S(T)$ domain.

For $\Omega = 2$, the entropy has no local extreme, as well. The coefficient a_2 does not appear in Eq. (14), thus in the case $a_2 > 0$ the entropy $S(T)$ monotonically increases with the temperature T and eventually saturates at the value

$$\bar{S} \approx k_B \left[1 - \ln \left(\frac{\hbar \sqrt{a_2}}{k_B} \right) \right]. \quad (15)$$

Remarkably, this value depends only on the $\omega(T)$ leading term coefficient a_2 and not on ω_0 . This behavior should be compared to the *localization* of the oscillator position X , Eq. (11). Contrary to $\text{Var}_X(T)$ the entropy $S(T)$ saturates, meaning that there is no *purification* of the state for the corresponding parameters, although there exists an upper bound on the oscillator entropy, Eq. (15). For a negative leading-term coefficient $a_2 < 0$ the entropy diverges at the temperature T_d at which the frequency vanishes, $\omega(T_d) = 0$. In such case the energy level spacing of the oscillator becomes negligible, causing flat-like population of the levels.

Finally, if $\Omega = 3$ and we assume negative leading-term coefficient $a_3 < 0$ there exist no $T_{\max} > 0$ for which the numerator of Eq. (14) vanishes, thus the entropy monotonically increases similarly to the position variance, see Fig. 2. Of course, the increase is faster compared to the standard oscillator with a constant frequency. For a positive leading-term coefficient $a_3 > 0$ the possible points of local extremes are the *positive real roots* of the cubic polynomial in Eq. (14). In the simplified case $a_1 \ll a_3 T^2$, the extreme appears at $T_{\max} \approx \sqrt[3]{2\omega_0^2/a_3}$, yielding the value according to Eq. (13)

$$S(T_{\max}) \approx k_B \left[1 - \ln \left(\frac{\hbar a_3^{1/3} \omega_0^{1/3}}{k_B} \right) \right], \quad (16)$$

approximately valid assuming the argument of the logarithm being large enough in accordance with Eq. (13). In this regime, we observe *purification* of the oscillator state with increasing temperature, even more unusual phenomena of strong coupling regime. Thus, in this case the thermal localization and purification appears in parallel. It is the best regime to jointly demonstrate both these counter-intuitive phenomena. For higher ω_0 the maximum appears at higher temperatures and $S(T_{\max})$ is reduced, see Eq. (16).

V. THE HEAT CAPACITIES

The counter-intuitive phenomena of thermal purification for the von Neumann entropy brought us close to thermodynamic analysis of strong coupling effects. In the classical macroscopic thermodynamics [45] heat capacities yield the amount of heat exchanged between a system and the heat bath when temperature changes during a specific thermodynamic process. For microscopic mechanical oscillator the heat exchange between the oscillator and its environment is hard to measure. In the present work we introduce two capacities (thermodynamic coefficients)

$$C_S(T) = T \frac{\partial S}{\partial T}, \quad (17)$$

$$C_U(T) = \frac{\partial \mathcal{U}}{\partial T}. \quad (18)$$

The measurement of the capacities (17) and (18) can provide us information about thermally activated microscopic processes in the system. In the weak coupling limit ($\lambda \rightarrow 0$, cf. Eq. (6)), $\omega(T) = \omega_0$ and these quantities are identical [45]. For the oscillator strongly coupled to the bath, each quantity provides a different information and each is a result of different type of possible (at least in principle) measurement.

First, the entropic capacity, $C_S(T)$, is obtained provided we can reconstruct the equilibrium state $\hat{\rho}(T)$, Eq. (5), of the oscillator strongly coupled to the bath and calculate the von Neumann entropy. It is experimentally accessible for many optomechanical and electromechanical experiments using the homodyne tomography [50]. In the case of an oscillator, different approach relying on the $\text{Var}_X(T)$ measurement is as well possible, being described at the end of this subsection.

Second, the heat capacity $C_U(T)$ is defined through the internal energy function $\mathcal{U}(T)$, given by the difference [19]

$$\mathcal{U}(T) = \langle \hat{H}_{\text{tot}} \rangle - \langle \hat{H}_B \rangle_B, \quad (19)$$

related to the Hamiltonian of mean force as [19]

$$\mathcal{U}(T) = \langle \hat{H}(T) \rangle - T \left\langle \frac{\partial \hat{H}}{\partial T} \right\rangle. \quad (20)$$

According to Eq. (19), the heat capacity $C_U(T)$ is an outcome of the differential calorimetric measurement. To see this, we note that the right hand side of Eq. (19) contains the energy difference between two independent systems: (i) the oscillator together with the bath, characterized by the total Hamiltonian \hat{H}_{tot} , cf. Eq. (4), and (ii) the plain bath without the oscillator with the Hamiltonian \hat{H}_B . Because the quantity $\mathcal{U}(T)$ is given by the difference of the average energies of the systems (i) and (ii), its change with temperature, $(\partial \mathcal{U} / \partial T) dT$, equals to the difference of energy flows into (i) and (ii). Hence, the capacity $C_U(T)$ can be obtained measuring the difference of energy flows into these two systems during temperature changes. It is not necessary to measure the state $\hat{\rho}(T)$ directly, however, it requires energy measurement with a rather high precision which is stimulating for further technological development [51–53].

The two capacities $C_S(T)$ and $C_U(T)$, can witness the fact that the interaction strength between the oscillator and the bath is beyond the weak-coupling limit. In this limit, both these capacities are strictly positive [45]. The negativity of the capacities reflects strong oscillator-bath coupling. We can formulate the following *strong-coupling witness*: If the respective capacity is negative, then, definitely, the system is strongly coupled to its surrounding. Moreover, the capacities can clearly identify the cases when the function $f(T)$, c.f. Eq. (2), is a nonlinear function of T .

A. The Capacity $C_S(T)$

The behavior of the entropic capacity $C_S(T) = T \partial S / \partial T$ is rather complex and interesting, cf. Fig. 4, and follows directly from Eq. (14). For the negative values of the leading-term coefficients $a_\Omega < 0$ the capacity diverges at same temperature T_d as the entropy. Figure 4 shows the capacity for the positive leading-term coefficients, $a_\Omega > 0$. For $\Omega \leq 2$, the capacity does not attain negative values as opposed to $\Omega = 3$. For larger temperatures, the three plotted curves approach the asymptotic values $C_S \approx k_B(1 - \Omega/2)$. The capacity $C_S(T)$ reaches its lowest values for the highest order of the nonlinearity in T , $\Omega = 3$. For smaller ω_0 , while other parameters are kept constant, the value $C_S(T) = 0$ is crossed at lower temperatures, allowing for easier observation of $C_S(T) < 0$. Negative capacity $C_S(T)$ means that the entropy of our system decreases with the increasing temperature.

In the classical regime, when both variances are far from the ground-state variance, the equilibrium probability density function factorizes, $\rho(X, P) = \rho(X)\rho(P)$. Then the von Neumann entropy can be decomposed into the position

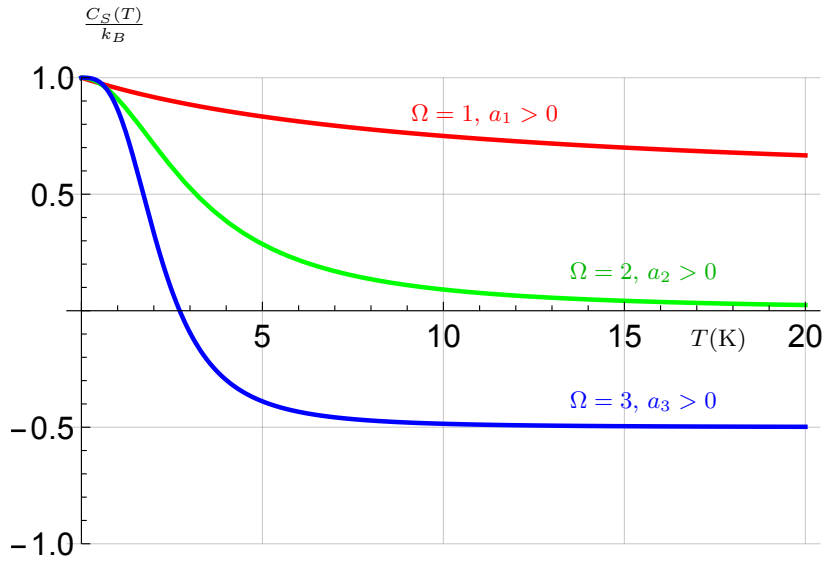


FIG. 4. The entropic capacity (17), for different values of Ω . For $\Omega \leq 2$, (red, green), $C_S(T)$ approach their asymptotic values $C_S(T) \approx k_B(1 - \Omega/2)$ according to Eq. (14). For $\Omega \geq 2$, $C_S(T)$ may become negative. In all plotted cases $m \approx 10^{-8}$ kg, $a_\Omega T \approx \omega_0^2$, $\omega_0 \approx 10^6$ rad/s [46]. The parameters used are the same as in Fig. 3.

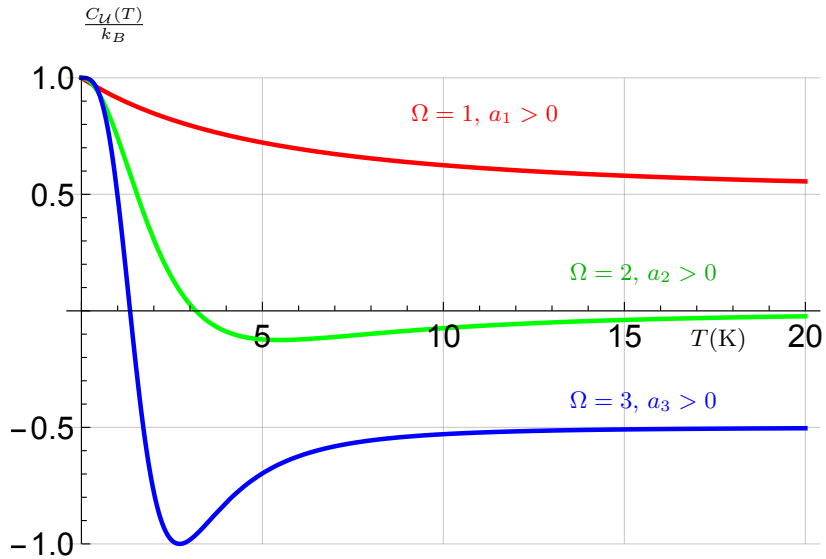


FIG. 5. The heat capacity (18) for different values of Ω . For $\Omega \geq 2$, $C_U(T)$ becomes negative and in all cases $C_U(T) \leq C_S(T)$, cf. Fig. 4. In all plotted cases $m \approx 10^{-8}$ kg, $a_\Omega T \approx \omega_0^2$, $\omega_0 \approx 10^6$ rad/s [46]. The parameters used are the same as in Fig. 4.

and momentum parts, $S(T) = S_X(T) + S_P(T)$, where $S_X(T) = -k_B \int dX \rho(X) \ln[\rho(X)]$, expresses the uncertainty of the probability density $\rho(X)$, and similarly for $S_P(T)$. The entropy $S_X(T)$ can be understood as a counterpart of the position variance $\text{Var}_X(T)$. Using $S(T) = S_X(T) + S_P(T)$, we obtain $C_S(T) = C_{S_X}(T) + C_{S_P}(T)$, cf. Eq (17). The momentum part contributes by the constant only, $C_{S_P}(T) = k_B/2$.

In analogy to the entropic capacity $C_{S_X}(T)$ we can define the mechanical position-uncertainty coefficient $C_{\text{Var}_X}(T) = T(\partial \text{Var}_X / \partial T)$. From a mechanical viewpoint, it determines a variance which can be reached by heating the oscillator up to a temperature T , if that variance constantly increases from $T = 0$ with a slope given by its local value $\partial \text{Var}_X / \partial T$. Its properties are different from $C_{S_X}(T)$. They are related as $C_{S_X}(T) = C_{\text{Var}_X}(T) / \text{Var}_X(T)$, thus $C_{\text{Var}_X}(T)$ can be used to determine $C_S(T)$, without the necessity of estimating the state $\hat{\rho}(T)$. In this way, localization of the particle can be directly measured and used to determine the main features of the capacity $C_S(T)$. In turn, this capacity can be used, in our case of an oscillator, to describe the properties of $C_U(T)$, discussed in the next subsection.

B. The Capacity $C_U(T)$

It turns out that the respective capacities $C_S(T)$ and $C_U(T)$ can be related to each other. For instance, we obtain the relation

$$C_U(T) = C_S(T) - T \frac{\partial}{\partial T} \left\langle \frac{\partial H}{\partial T} \right\rangle, \quad (21)$$

yielding another useful result valid for our HMF (3)

$$C_U(T) = \frac{\partial}{\partial T} [T C_S(T)]. \quad (22)$$

Clearly, in the weak-coupling limit $C_U(T)$ and $C_S(T)$ are identical.

Eq. (22) allows for determination of $C_U(T)$ from $C_S(T)$, achievable by homodyne tomography [22], or even from the knowledge of $\text{Var}_X(T)$, see Sec. V A. The behavior of $C_U(T)$ for different values of Ω is shown in Fig. 5, for the same parameter values as used in Fig. 4.

Fig. 5 illustrates that $C_U(T)$ can serve for an even more interesting purpose. Surprisingly, it can witness the order Ω of the temperature dependence $\omega(T)$ in a more effective way compared to $C_S(T)$, due to the relation $C_U(T) \leq C_S(T)$. Thus from the behavior of $C_U(T)$ we can determine whether the temperature dependence in (2) is linear or of a higher order in T . It simultaneously implies, that to reach a strong coupling proved by negative capacity $C_U(T)$, $\omega(T)$ with $\Omega \geq 2$, Eq. (2), is required.

Finally, note that in Refs. [54, 55] we studied the HMF where the temperature dependence was in the *linear* additive term $f(T)\hat{X}$, in contrast to the quadratic term $f(T)\hat{X}^2$ in the present Eq. (3). Such linear term does not lead to $C_U(T) < 0$ or $C_S(T) < 0$ for any $\Omega \leq 3$, assuming we adopt the same form of $\omega(T)$ as in Eq. (2). The behavior of the capacity does strongly depend on the particular form of the HMF.

In analogy with classical weak-coupling thermodynamics, one can be tempted to define the third capacity as $C_H(T) = \partial \langle \hat{H} \rangle / \partial T$, with $\langle \hat{H} \rangle$ being the mean value of the HMF, Eq. (3). This quantity is not related to a heat flow between the bath and the oscillator and has no abilities to witness localization and/or purification of the oscillator when the surrounding temperature is changed. However, this quantity resembles the textbook results for the harmonic oscillator heat capacity $C_H(T) = k_B$, valid in the weak coupling limit [45]. Only in this limit, $\langle \hat{H} \rangle$ has the meaning of the average energy of the system and $C_H(T)$ coincides with the capacities defined in Eqs. (17), (18).

VI. ROUTE TO AN EXPERIMENT

We can envisage a possible experiment capable to demonstrate the results presented in this paper. An important condition that has to be met is that the effect of the non-negligible system-bath interaction on the bare system would result into the form of the HMF $\hat{H}(T)$ given in Eq. (3). In a high-temperature regime experiments we can encounter a wide variety of qualitatively different behaviors regarding the oscillator localization (reduction of its position variance) and the purification (reduction of its von Neumann entropy) or other quantities. The main result of our paper is that for at most *linear* temperature dependence of the square of the oscillator frequency we can not observe any of these effects. On contrary, for the *cubic* temperature dependence of the frequency both effects appear simultaneously and are more pronounced with increasing temperature, cf. Figs. 2-3. Regarding the frequency ranges well suitable for the observation of interesting effects described in this paper, we conclude the following. When localization (Sec. III), state purification (Sec. IV), and/or witnessing strong coupling to the bath (Sec. V) are in the focus of interest, it is preferable to employ lower bare frequency oscillators. On the other hand, if the figure of merit is to keep the oscillator in the low-entropy regime one should preferably work with a higher bare frequency oscillators.

In the future, it can be interesting to analyze performance of quantum heat engines at strong coupling [56–60] using the present phenomenological approach.

ACKNOWLEDGMENTS

M.K. and R.F. acknowledge the support of the project GB14-36681G of the Czech Science Foundation. A.R. gratefully acknowledges support of the project No. 17-06716S of the Czech Science Foundation. R.F. acknowledges

project TheBlinQC of Quanterra EU program co-financed by the Ministry of Education, Science and Youth of Czech Republic. A.R. and M.K. are grateful to P. Cabišová for stimulating discussions.

-
- [1] M. Aspelmeyer, T. J. Kippenberg, and F. Marquardt, “Cavity optomechanics,” *Rev. Mod. Phys.* **86**, 1391–1452 (2014).
- [2] K. Zhang, F. Bariani, and P. Meystre, “Quantum optomechanical heat engine,” *Phys. Rev. Lett.* **112**, 150602 (2014).
- [3] Wang D. Y., Bai C. H., Wang H. F., Zhu A. D., and Zhang S., “Steady-state mechanical squeezing in a double-cavity optomechanical system,” *Sci. Rep.* **6**, 38559 (2016).
- [4] P. Grangier, R. E. Slusher, B. Yurke, and A. LaPorta, “Squeezed-light-enhanced polarization interferometer,” *Phys. Rev. Lett.* **59**, 2153–2156 (1987).
- [5] M. Hossein-Zadeh and K. J. Vahala, “An optomechanical oscillator on a silicon chip,” *IEEE Journal of Selected Topics in Quantum Electronics* **16**, 276–287 (2010).
- [6] S. Zaitsev, O. Gottlieb, and E. Buks, “Nonlinear dynamics of a microelectromechanical mirror in an optical resonance cavity,” *Nonlinear Dynamics* **69**, 1589–1610 (2012).
- [7] D. Yuvaraj, M. B. Kadam, O. Shtempluck, and E. Buks, “Optomechanical cavity with a buckled mirror,” *Journal of Microelectromechanical Systems* **22**, 430–437 (2013).
- [8] B. Khanaliloo, H. Jayakumar, A. C. Hryciw, D. P. Lake, H. Kaviani, and P. E. Barclay, “Single-crystal diamond nanobeam waveguide optomechanics,” *Phys. Rev. X* **5**, 041051 (2015).
- [9] N. R. Jungwirth, B. Calderon, Y. Ji, M. G. Spencer, M. E. Flatt, and G. D. Fuchs, “Temperature dependence of wavelength selectable zero-phonon emission from single defects in hexagonal boron nitride,” *Nano Letters* **16**, 6052–6057 (2016).
- [10] A. K. Pandey, O. Gottlieb, O. Shtempluck, and E. Buks, “Performance of an aupd micromechanical resonator as a temperature sensor,” *Applied Physics Letters* **96**, 203105 (2010).
- [11] R. de Miguel, “Temperature-dependent energy levels and size-independent thermodynamics,” *Phys. Chem. Chem. Phys.* **17**, 15691–15693 (2015).
- [12] Ch. Jarzynski, “Nonequilibrium work theorem for a system strongly coupled to a thermal environment,” *J. Stat. Mech.* **2004**, P09005 (2004).
- [13] M. F. Gelin and M. Thoss, “Thermodynamics of a subensemble of a canonical ensemble,” *Phys. Rev. E* **79**, 051121 (2009).
- [14] M. Esposito, K. Lindenberg, and Ch. Van den Broeck, “Entropy production as correlation between system and reservoir,” *New J. Phys.* **12**, 013013 (2010).
- [15] T. G. Philbin and J. Anders, “Thermal energies of classical and quantum damped oscillators coupled to reservoirs,” *J. Phys. A: Math. Theor.* **49**, 215303 (2016).
- [16] Ch. Jarzynski, “Stochastic and macroscopic thermodynamics of strongly coupled systems,” *Phys. Rev. X* **7**, 011008 (2017).
- [17] P. Strasberg and M. Esposito, “Stochastic thermodynamics in the strong coupling regime: An unambiguous approach based on coarse graining,” *Phys. Rev. E* **95**, 062101 (2017).
- [18] U. Seifert, “First and second law of thermodynamics at strong coupling,” *Phys. Rev. Lett.* **116**, 020601 (2016).
- [19] P. Talkner and P. Hänggi, “Open system trajectories specify fluctuating work but not heat,” *Phys. Rev. E* **94**, 022143 (2016).
- [20] G. S. Rushbrooke, “On the statistical mechanics of assemblies whose energy-levels depend on the temperature,” *Trans. Faraday Soc.* **36**, 1055–1062 (1940).
- [21] E. W. Elcock and P. T. Landsberg, “Temperature dependent energy levels in statistical mechanics,” *Proceedings of the Physical Society. Section B* **70**, 161 (1957).
- [22] M. R. Vanner, I. Pikovski, G. D. Cole, M. S. Kim, Č. Brukner, K. Hammerer, G. J. Milburn, and M. Aspelmeyer, “Pulsed quantum optomechanics,” *Proceedings of the National Academy of Sciences* **108**, 16182–16187 (2011).
- [23] D. I. Bower, *An Introduction to Polymer Physics* (Cambridge University Press, 2002).
- [24] A. Radkowsky, “Temperature dependence of electron energy levels in solids,” *Phys. Rev.* **73**, 749–761 (1948).
- [25] H. Y. Fan, “Temperature dependence of the energy gap in semiconductors,” *Phys. Rev.* **82**, 900–905 (1951).
- [26] D. Emin, “Effect of temperature-dependent energy-level shifts on a semiconductor’s peltier heat,” *Phys. Rev. B* **30**, 5766–5770 (1984).
- [27] A. Aldea, “The thermopower of non-localized electrons in amorphous semiconductors,” *Journal of Non-Crystalline Solids* **114**, 375 (1989).
- [28] R. J. Donnelly and P. H. Roberts, “A theory of temperature-dependent energy levels: Thermodynamic properties of He II,” *Journal of Low Temperature Physics* **27**, 687–736 (1977).
- [29] O. Shental and I. Kanter, “Shannon meets carnot: Generalized second thermodynamic law,” *EPL (Europhysics Letters)* **85**, 10006 (2009).
- [30] M. Cardona and R. K. Kremer, “Temperature dependence of the electronic gaps of semiconductors,” *Thin Solid Films* **571**, 680 – 683 (2014).
- [31] Y. Takuya, “Efficiencies of thermodynamics when temperature-dependent energy levels exist,” *Phys. Chem. Chem. Phys.* **18**, 7011–7014 (2016).
- [32] C. E. P. Villegas, A. R. Rocha, and A. Marini, “Anomalous temperature dependence of the band gap in black phosphorus,” *Nano Letters* **16**, 5095–5101 (2016).

- [33] R. de Miguel and J. M. Rubí, “Thermodynamics far from the thermodynamic limit,” *The Journal of Physical Chemistry B* **121**, 10429–10434 (2017).
- [34] Y. A. Mitropolskii and N. Van Dao, *Applied Asymptotic Methods in Nonlinear Oscillations* (Springer, 1997).
- [35] F. J. Giessibl, “Forces and frequency shifts in atomic-resolution dynamic-force microscopy,” *Phys. Rev. B* **56**, 16010–16015 (1997).
- [36] H. Hölscher, B. Gotsmann, W. Allers, U. D. Schwarz, H. Fuchs, and R. Wiesendanger, “Measurement of conservative and dissipative tip-sample interaction forces with a dynamic force microscope using the frequency modulation technique,” *Phys. Rev. B* **64**, 075402 (2001).
- [37] J. G. Kirkwood, “Statistical mechanics of fluid mixtures,” *J. Chem. Phys.* **3**, 300 (1935).
- [38] B. Roux and T. Simonson, “Implicit solvent models,” *Biophys. Chem.* **78**, 1 – 20 (1999).
- [39] D. Chandler, *Introduction to Modern Statistical Mechanics*, 1st ed. (Oxford University Press, 1987).
- [40] G. W. Ford, J. T. Lewis, and R. F. O’Connell, “Quantum oscillator in a blackbody radiation field,” *Phys. Rev. Lett.* **55**, 2273–2276 (1985).
- [41] G. W. Ford, J. T. Lewis, and R. F. O’Connell, “Quantum oscillator in a blackbody radiation field ii. direct calculation of the energy using the fluctuation-dissipation theorem,” *Ann. Phys.* **185**, 270 – 283 (1988).
- [42] G. W. Ford and R. F. O’Connell, “Quantum thermodynamic functions for an oscillator coupled to a heat bath,” *Phys. Rev. B* **75**, 134301 (2007).
- [43] P. Hänggi, G.-L. Ingold, and P. Talkner, “Finite quantum dissipation: the challenge of obtaining specific heat,” *New. J. Phys.* **10**, 115008 (2008).
- [44] G.-L. Ingold, P. Hänggi, and P. Talkner, “Specific heat anomalies of open quantum systems,” *Phys. Rev. E* **79**, 061105 (2009).
- [45] W. Greiner, L. Neise, and Stöcker H., “Thermodynamics and statistical mechanics,” (Springer-Verlag, Berlin, 1997).
- [46] G. D. Cole, I. Wilson-Rae, K. Werbach, M. R. Vanner, and M. Aspelmeyer, “Phonon-tunnelling dissipation in mechanical resonators,” *Nature Communications* **2**, 231 (2011).
- [47] M. Aspelmeyer, P. Meystre, and K. Schwab, “Quantum optomechanics,” *Phys. Today* **65**, 29 (2012).
- [48] W. H. Zurek, “Decoherence, einselection, and the quantum origins of the classical,” *Rev. Mod. Phys.* **75**, 715–775 (2003).
- [49] P. J. Coles, M. Berta, M. Tomamichel, and S. Wehner, “Entropic uncertainty relations and their applications,” *Rev. Mod. Phys.* **89**, 015002 (2017).
- [50] G. A. Brawley, M. R. Vanner, P. E. Larsen, S. Schmid, A. Boisen, and W. P. Bowen, “Nonlinear optomechanical measurement of mechanical motion,” *Nature Communications* **7**, 10988 (2016).
- [51] J. P. Pekola, P. Solinas, A. Shnirman, and D. V. Averin, “Calorimetric measurement of work in a quantum system,” *New Journal of Physics* **15**, 115006 (2013).
- [52] S. Gasparinetti, K. L. Viisanen, O. P. Saira, T. Faivre, M. Arzeo, M. Meschke, and J. P. Pekola, “Fast electron thermometry for ultrasensitive calorimetric detection,” *Phys. Rev. Applied* **3**, 014007 (2015).
- [53] J. Govenius, R. E. Lake, K. Y. Tan, and M. Möttönen, “Detection of zeptojoule microwave pulses using electrothermal feedback in proximity-induced josephson junctions,” *Phys. Rev. Lett.* **117**, 030802 (2016).
- [54] M. Kolář, A. Ryabov, and R. Filip, “Optomechanical oscillator controlled by variation in its heat bath temperature,” *Phys. Rev. A* **95**, 042105 (2017).
- [55] M. Kolář, A. Ryabov, and R. Filip, “Extracting work from quantum states of radiation,” *Phys. Rev. A* **93**, 063822 (2016).
- [56] R. Gallego, A. Riera, and J. Eisert, “Thermal machines beyond the weak coupling regime,” *New J. Phys.* **16**, 125009 (2014).
- [57] D. Gelbwaser-Klimovsky and A. Aspuru-Guzik, “Strongly coupled quantum heat machines,” *J. Phys. Chem. Lett.* **6**, 3477–3482 (2015).
- [58] G. Katz and R. Kosloff, “Quantum thermodynamics in strong coupling: Heat transport and refrigeration,” *Entropy* **18**, 186 (2016).
- [59] D. Newman, F. Mintert, and A. Nazir, “Performance of a quantum heat engine at strong reservoir coupling,” *Phys. Rev. E* **95**, 032139 (2017).
- [60] M. Perarnau-Llobet, H. Wilming, A. Riera, R. Gallego, and J. Eisert, “Strong coupling corrections in quantum thermodynamics,” *Phys. Rev. Lett.* **120**, 120602 (2018).